

# Surprising luminescent properties of the polyphosphates Ln(PO<sub>3</sub>)<sub>3</sub> : Eu (Ln = Y, Gd, Lu)<sup>†</sup>

Henning A. Höppe,<sup>\*a</sup> Karolina Kazmierczak,<sup>b</sup> Sylwia Kacprzak,<sup>c</sup> Inga Schellenberg<sup>d</sup> and Rainer Pöttgen<sup>d</sup>

The optical emission properties of the lanthanoid catena-polyphosphates Ln(PO<sub>3</sub>)<sub>3</sub> (Ln = Y, Gd, Lu) doped with europium were investigated. Incommensurately modulated β-Y(PO<sub>3</sub>)<sub>3</sub> : Eu (super space group *Cc* (0|0.364|0)0) and Gd(PO<sub>3</sub>)<sub>3</sub> : Eu (space group *I2/a*) show the usual emission characteristics of Eu<sup>3+</sup>, while in Lu(PO<sub>3</sub>)<sub>3</sub> : Eu (space group *Cc*) the europium is unprecedentedly partially reduced to the divalent state, as proven by both a broad emission band at 406 nm excited at 279 nm and an EPR spectroscopic investigation. <sup>151</sup>Eu-Mössbauer spectroscopy showed that only a very small part of the europium is reduced in Lu(PO<sub>3</sub>)<sub>3</sub> : Eu. An explanation for this unusual behaviour is given.

## 1. Introduction

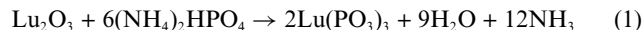
Crystalline compounds of rare-earth metals with condensed anions are of broad interest as possible host structures useful for optical applications. The targets are phosphors for white LEDs, quantum cutting phosphors to replace mercury plasma tubes by xenon plasma tubes, as upconversion phosphors in solar cells or as host structures for scintillators.<sup>1</sup>

In recent contributions, we have shed light on the crystal chemistry of the polyphosphates Ln(PO<sub>3</sub>)<sub>3</sub> with Ln = Sc, Y, Gd...Lu.<sup>2,3</sup> While Lu(PO<sub>3</sub>)<sub>3</sub> and Gd(PO<sub>3</sub>)<sub>3</sub> adopt normally-ordered non-centrosymmetric and centrosymmetric crystal structures, respectively, the structures of the phosphates Ln(PO<sub>3</sub>)<sub>3</sub> with Ln = Y, Tb...Yb are incommensurately modulated at room temperature, *i.e.*, non-centrosymmetric β-Ln(PO<sub>3</sub>)<sub>3</sub>. Therefore, these polyphosphates allow a comparison of the fluorescence in very similar host structures that are only different in the size of the crystallographic site and the crystal symmetry.

Herein, we present a comparison of these polyphosphates doped with europium to clarify the influence of crystal symmetry on the optical properties. In the case of Lu(PO<sub>3</sub>)<sub>3</sub> : Eu, which showed unexpected behaviour, the optical spectroscopic investigations were supported by electron paramagnetic resonance (EPR) and Mössbauer spectroscopy to clarify the valence state of the Eu.

## 2. Experimental section

Doped phosphates Ln(PO<sub>3</sub>)<sub>3</sub> with Ln = Y, Gd, Lu were synthesised according to eqn (1) starting from ammonium hydrogen phosphate and the respective lanthanide oxides.



A typical synthesis starts with a mixture of 101.7 mg (0.2556 mmol) lutetium oxide (ChemPur, 99.9%), 4.9 mg (0.014 mmol) europium oxide (ChemPur, 99.9%) and 226.1 mg (1.712 mmol) diammonium hydrogenphosphate (ABCR, 98%), which were transferred into an alumina crucible. The latter was then heated to 873 K at a rate of 180 K h<sup>-1</sup> and maintained at this temperature for 12 h. After cooling to room temperature at a rate of 180 K h<sup>-1</sup>, 206 mg (0.500 mmol, 97.8%) Lu(PO<sub>3</sub>)<sub>3</sub> : Eu was obtained as a crystalline, colourless and non-hygroscopic powder.

### X-ray powder diffractometry

The crystalline samples were enclosed in glass capillaries of 0.2 mm diameter and investigated at room temperature in the Debye–Scherrer geometry on a STOE Stadi P powder diffractometer with Ge(111)-monochromatized Mo-Kα radiation (linear PSD detector, step width 0.5°, acquisition time: 90 s step<sup>-1</sup>). The obtained crystalline products were phase pure according to X-ray powder diffractometry (for Lu(PO<sub>3</sub>)<sub>3</sub> : Eu see Fig. 1).

### Luminescence spectroscopy

Luminescence spectra were recorded at room temperature on a Perkin-Elmer LS55 fluorescence spectrometer equipped with a Xe discharge lamp (equivalent to 20 kW for 8 μs duration) and a gated photomultiplier with a modified S5 response. Spectra were corrected for excitation and emission.

<sup>a</sup>Institut für Physik, Universität Augsburg, Universitätsstraße 1, D-86159, Augsburg, Germany. E-mail: henning@ak-hoeppe.de; Fax: +49 821-598-3032

<sup>b</sup>Institut für Anorganische und Analytische Chemie, Universität Freiburg, Albertstraße 21, D-79104, Freiburg im Breisgau, Germany

<sup>c</sup>Institut für Physikalische Chemie, Universität Freiburg, Albertstraße 21, D-79104, Freiburg im Breisgau, Germany

<sup>d</sup>Institut für Anorganische und Analytische Chemie, Universität Münster, Corrensstraße 30, D-48149, Münster, Germany

<sup>†</sup>Electronic supplementary information (ESI) available. See DOI: 10.1039/c1dt10043b

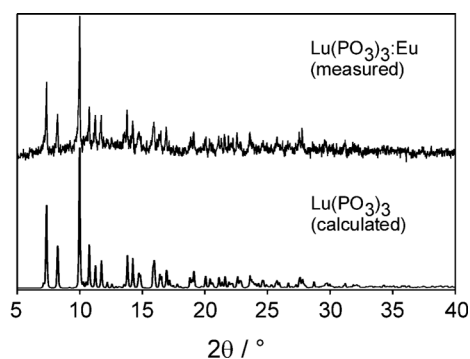


**Fig. 1** Comparison of a measured diffraction pattern of  $\text{Lu}(\text{PO}_3)_3:\text{Eu}$  (above) and a calculated powder diffraction pattern of  $\text{Lu}(\text{PO}_3)_3$  (below).

### EPR spectroscopy

X-Band (9.411 GHz) continuous wave (cw) EPR data were obtained using a Bruker EMX spectrometer equipped with a Bruker ER 4122SHQE resonator. An Oxford helium gas flow cryostat (ESR-900) was used for sample cooling. The temperature was regulated to  $\pm 0.1$  K by an Oxford ITC-503S temperature controller. The X-band EPR spectra were recorded at 10 K. Q-Band (34.122 GHz) cw-EPR spectra were recorded with a Bruker ESP380E spectrometer equipped with a cylindrical resonator (Bruker ER 5106 QT-W1) immersed in a helium gas flow cryostat (Oxford CF-935). The temperature was regulated to  $\pm 0.1$  K by an Oxford temperature controller (ITC-503). The Q-band spectra were recorded at 20 K. The sample was filled into synthetic silica glass tubes of 3 mm inner diameter for X-band EPR and 1 mm inner diameter for Q-band EPR experiments.

### $^{151}\text{Eu}$ Mössbauer spectroscopy

The 21.53 keV transition of  $^{151}\text{Eu}$  with an activity of 130 MBq (2% of the total activity of a  $^{151}\text{Sm}:\text{EuF}_3$  source) was used for the Mössbauer spectroscopic experiments, which were conducted in the usual transmission geometry. The measurements were performed with a commercial helium bath cryostat. The temperature of the absorber was varied between 4.2 K and room temperature, while the source was kept at room temperature. The temperature was controlled by a resistance thermometer ( $\pm 0.5$  K accuracy). The sample was enclosed in a small PVC container at a thickness corresponding to about  $10 \text{ mg Eu cm}^{-2}$ .

## 3. The crystal structures of $\beta\text{-Y}(\text{PO}_3)_3$ , $\text{Gd}(\text{PO}_3)_3$ and $\text{Lu}(\text{PO}_3)_3$

The crystal structures of the title compounds can be derived from the basic unit cell of the incommensurately modulated phases, as previously described.<sup>2,3</sup>

### Basic structure

The crystal structure consists of infinite zig-zag chains of  $\text{PO}_4$  tetrahedra connected by common corners, giving the polyphosphate anion  $\text{PO}_3^-$ . In-between these chains, the lanthanide atoms are positioned and coordinated by six terminal oxygen atoms, forming a slightly distorted octahedron. Fig. 2 illustrates the unit cell of the basic structure.

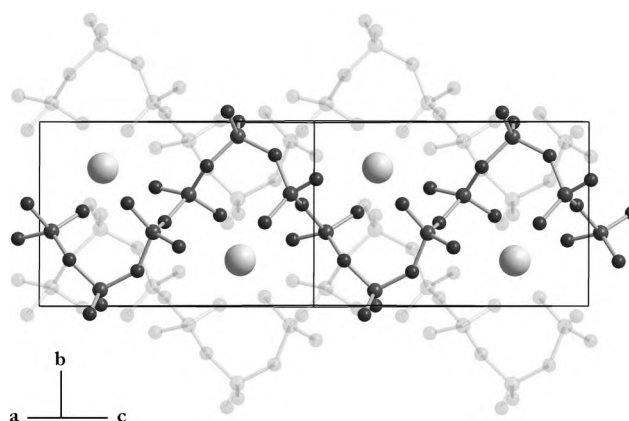


**Fig. 2** Representation of the basic structure; two of the three phosphate chains are in the background (shaded), the  $\text{Ln}^{3+}$  cations are shown as large grey spheres.

### Modulated structure of $\beta\text{-Y}(\text{PO}_3)_3$

The room temperature form,  $\beta\text{-Y}(\text{PO}_3)_3$ , exhibits an incommensurately modulated crystal structure in super space group  $Cc$  ( $0|0.364|0$ ). Considering the modulation vector  $\mathbf{q} = 0.364\mathbf{b}^*$ , the positions of all the atoms obey sinusoidal modulation waves. Below 180 K, the low temperature commensurate form,  $\alpha\text{-Y}(\text{PO}_3)_3$ , is formed.<sup>3</sup>

### Crystal structure of $\text{Lu}(\text{PO}_3)_3$

$\text{Lu}(\text{PO}_3)_3$  crystallises isotypically with C-type phosphates<sup>4</sup> in the space group  $Cc$  and adopts a three-fold superstructure along  $\mathbf{b}$  of the above-described basic structure, as shown in Fig. 5 and Fig. S1 (ESI†).

### Crystal structure of $\text{Gd}(\text{PO}_3)_3$

$\text{Gd}(\text{PO}_3)_3$  can be described in terms of a four-fold superstructure of the basic structure, generating an inversion centre, leading to the centrosymmetric space group  $I2/a$ , as represented in Fig. S1 (ESI†).

## 4. Luminescence of $\text{Y}(\text{PO}_3)_3:\text{Eu}$ and $\text{Gd}(\text{PO}_3)_3:\text{Eu}$

As can be easily seen from Fig. 3, yttrium and gadolinium polyphosphate doped with europium show the normal emission characteristics of  $\text{Eu}^{3+}$ . Their solid state emission spectra were investigated at room temperature. Both compounds exhibit several strong characteristic emission bands for isolated europium(III) ions in the visible region excited at 209 nm ( $\beta\text{-Y}(\text{PO}_3)_3:\text{Eu}$ ) via the well known charge-transfer or reduction band of  $\text{Eu}^{3+}$ , which occurs at a slightly shorter wavelength compared with the CT band found in  $\text{YPO}_4:\text{Eu}^{3+}$  at 223 nm.<sup>5</sup>  $\text{Gd}(\text{PO}_3)_3:\text{Eu}$  is excited at 274 nm via a direct transition of  $\text{Gd}^{3+}$  ( $^8\text{S}_{7/2} \rightarrow ^6\text{I}_{11/2}$ ). The bands and their respective transition assignments are found in Table 1. Both host structures can be doped easily with  $\text{Eu}^{3+}$  since the charge and size of the replaced cations are comparable (radii for coordination number 6:  $r(\text{Y}^{3+}) = 90 \text{ pm}$ ,  $r(\text{Gd}^{3+}) = 94 \text{ pm}$  and  $r(\text{Eu}^{3+}) = 95 \text{ pm}$ ).<sup>6</sup>

The main difference in the emission spectra is the intensity ratio of the  $^5\text{D}_0 \rightarrow ^7\text{F}_1$  emission to the hypersensitive transition  $^5\text{D}_0 \rightarrow ^7\text{F}_2$ , which is subject to different site environments.<sup>7</sup> Moreover, the

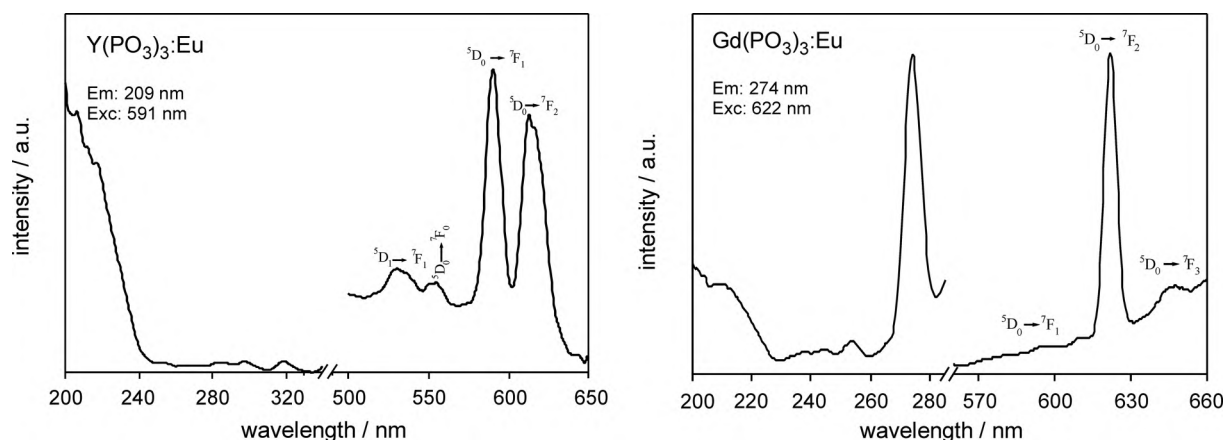


Fig. 3 Excitation and emission spectra of  $\text{Y}(\text{PO}_3)_3:\text{Eu}$  (left) and  $\text{Gd}(\text{PO}_3)_3:\text{Eu}$  (right).

**Table 1** Assignment of the emission bands of  $\beta\text{-Y}(\text{PO}_3)_3:\text{Eu}$  and  $\text{Gd}(\text{PO}_3)_3:\text{Eu}$

	$\beta\text{-Y}(\text{PO}_3)_3:\text{Eu}^{3+}$		$\text{Gd}(\text{PO}_3)_3:\text{Eu}^{3+}$	
	$\lambda/\text{nm}$	$E/10^3\text{ cm}^{-1}$	$\lambda/\text{nm}$	$E/10^3\text{ cm}^{-1}$
$^5\text{D}_0 \rightarrow ^7\text{F}_2$	531	18.8	—	—
$^5\text{D}_0 \rightarrow ^7\text{F}_0$	555	18.0	—	—
$^5\text{D}_0 \rightarrow ^7\text{F}_1$	591	16.9	595	16.8
$^5\text{D}_0 \rightarrow ^7\text{F}_2$	613	16.3	611	16.3
$^5\text{D}_0 \rightarrow ^7\text{F}_3$	—	—	622	16.1
			648	15.4

presence of the  $^5\text{D}_0 \rightarrow ^7\text{F}_0$  transition in the yttrium compound is in accordance with the slightly distorted octahedral symmetry of the yttrium site.

The excitation of both phosphors may occur *via* an allowed O $\rightarrow$ Eu charge-transfer transition for  $\beta\text{-Y}(\text{PO}_3)_3:\text{Eu}$  (onset at 245 nm) and  $\text{Gd}(\text{PO}_3)_3:\text{Eu}$  (onset at 231 nm), or by the excitation of gadolinium ( $^8\text{S}_{7/2} \rightarrow ^6\text{I}_{11/2}$  transition at 274 nm). As expected, the charge-transfer of  $\text{Eu}^{3+}$  occurs at similar energies in both compounds.<sup>8</sup>

## 5. Luminescence of $\text{Lu}(\text{PO}_3)_3:\text{Eu}$

In contrast to the other doped polyphosphates,  $\text{Lu}(\text{PO}_3)_3:\text{Eu}$  does not show any trace of  $\text{Eu}^{3+}$  emissions but comprises a broad emission band peaking at 406 nm with an additional shoulder (Fig. 4). Broad emissions are typical for d–f transitions, as found in divalent europium. In  $\text{Lu}(\text{PO}_3)_3:\text{Eu}$ , these emissions are best excited at 280 nm according to the excitation spectrum (Fig. 4, left). In contrast to f–f transitions, f–d transitions react due to the participation of d levels that are very sensitive to their coordination environment. Typical values found for phosphates are 404 nm in  $\alpha\text{-Sr}(\text{PO}_3)_2:\text{Eu}^0$  or 375 nm in  $\text{Ba}(\text{PO}_3)_2:\text{Eu}$ .<sup>10</sup> During the synthesis in air, the trivalent europium ions were at least partially reduced *in situ*.

### 5.1 A spontaneous reduction of $\text{Eu}^{3+}$ to $\text{Eu}^{2+}$

This *in situ* reduction is highly unprecedented behaviour since the syntheses were carried out in air at 600 °C, the same conditions that the other two compounds were exposed to. Moreover,

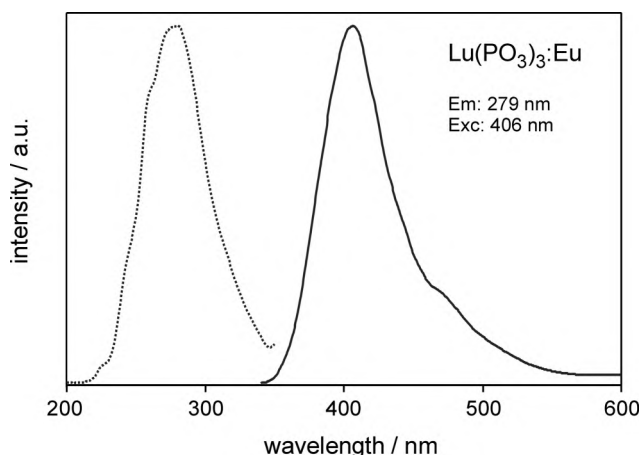
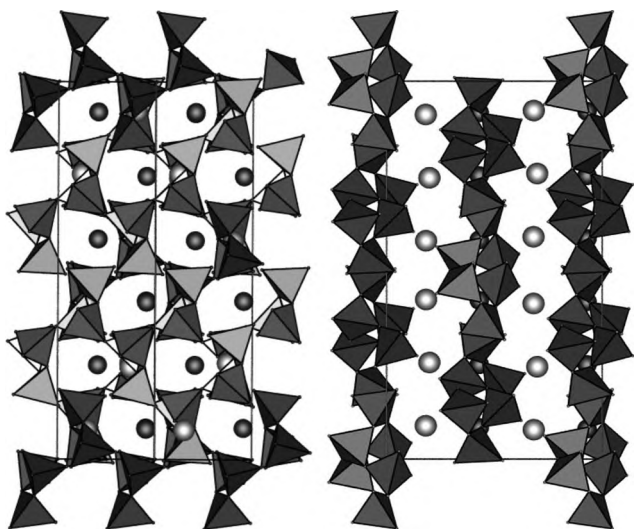


Fig. 4 Excitation and emission spectra of  $\text{Lu}(\text{PO}_3)_3:\text{Eu}$ .

reducing agents like hydrogen normally have to be applied to make europium reduce from the more stable trivalent state to the divalent one. In the literature, such *in situ* reductions of europium are rarely found. If  $\text{SrB}_4\text{O}_7$  is doped with trivalent Eu or Sm in air, the divalent ions are found.<sup>11</sup> In this case, the authors ascribed this unusual behaviour to the fact that the host material does not contain any oxidizing ions, and additionally provides crystallographic sites suitable for the reduction to  $\text{Eu}^{2+}$  and  $\text{Sm}^{2+}$ . They also stated that the cation to be substituted should have a radius similar to that of the divalent rare earth ion and that the host should consist of rigid tetrahedral units such as  $\text{BO}_4$ ,  $\text{SO}_4$  or  $\text{PO}_4$ .<sup>11</sup> In our case, most of the preconditions are fulfilled—we even provide slightly reducing ammonium ions during the synthesis—except for the fact that  $\text{Lu}^{3+}$  is significantly smaller than  $\text{Eu}^{3+}$  ( $r(\text{Lu}^{3+}) = 85\text{ pm}$  and  $r(\text{Eu}^{3+}) = 95\text{ pm}$ )<sup>6</sup> and, of course,  $\text{Eu}^{2+}$  ( $r_{\text{c.n.}=6}(\text{Eu}^{2+}) = 117\text{ pm}$  and  $r_{\text{c.n.}=8}(\text{Eu}^{2+}) = 125\text{ pm}$ ).<sup>6</sup>

Consequently, the  $\text{Eu}^{3+}$  ions are too large compared with the  $\text{Lu}^{3+}$  present in the host structure, and apparently the site size cannot be customised for the europium ions. Therefore, the europium ions evade from the Lu positions in the crystal structure to nearby voids present in the crystal structure presented in Fig. 5. These are located at the approximate coordinates 0.93/*y*/0.16 (*y*  $\approx$  0.08, 0.42, 0.75) with respect to the setting of  $\text{Lu}(\text{PO}_3)_3$  in  $Cc$ .<sup>2</sup> We initially localised these voids by simply looking at



**Fig. 5** Crystal structure of  $\text{Lu}(\text{PO}_3)_3$  viewed approximately along  $[1\ 0\ 1]$  (left) and along  $c$  ( $b$  up) (right); the  $\text{PO}_4$  tetrahedra are shown as closed polyhedra, light grey spheres represent Lu atoms and dark grey spheres show the possible voids in the crystal structure.

the structure. The later found possible positions were calculated by centring of the coordination polyhedra using the program DIAMOND.<sup>12</sup> Finally, these voids were checked for electrostatic reasonability using calculations based on the MAPLE concept (MAPLE = Madelung Part of Lattice Energy).<sup>13-15</sup> According to these calculations, the voids correspond to a local Madelung potential typical for divalent ions.

The voids can apparently react more flexibly to the presence of a larger ion. Moreover, they are seven-fold coordinated, which is a more common coordination number of the lighter trivalent lanthanide ions and especially of the larger divalent ones. The original Lu site is only octahedrally coordinated.

A similar situation is found in the thiogallate  $\text{ZnGa}_2\text{S}_4 : \text{Eu}^{2+}$ , where the divalent europium ions are presumably not located on the original zinc sites but in nearby octahedral voids because the  $\text{Zn}^{2+}$  cations are much smaller than the europium ions.<sup>16</sup>

The voids have a distance of around 3 Å to the adjacent Lu sites (Fig. 6). An advantage is the fact that, per regular site, two voids can be occupied with a distance of more than 5 Å between them. This gives the chance to compensate for the lost positive charges. Three  $\text{Eu}^{2+}$  have to replace two  $\text{Lu}^{3+}$ . This is supported by the occurrence of two distinct emissions. One is attributed to a single-filled void and the other to two simultaneously occupied voids with interactions of  $\text{Eu}^{2+}/\text{Lu}^{3+}$

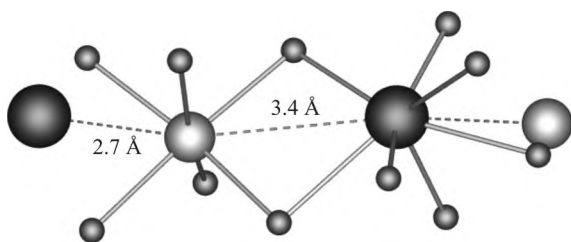


**Fig. 6** Surrounding of the Lu atoms represented as light grey spheres and the voids shown as dark grey spheres, respectively (distances in Å); the small grey spheres represent oxygen atoms.

or  $\text{Eu}^{2+}/\text{Eu}^{2+}$ . At this point, this question cannot be clarified though.

## 5.2 EPR spectroscopy of $\text{LuP}_3\text{O}_9 : \text{Eu}$

In contrast to  $\text{Eu}^{3+}$  ( $4f^6$ ,  $S = 3$ ),  $\text{Eu}^{2+}$  ( $4f^7$ ,  $S = 7/2$ ) can be easily detected by electron paramagnetic resonance (EPR) spectroscopy. No EPR signal is expected for  $\text{Eu}^{3+}$  with its  $J = 0$  ground state.<sup>17</sup> Fig. 7 shows the X-band (A) and Q-band (B) EPR spectra of europium-doped  $\text{LuP}_3\text{O}_9 : \text{Eu}$  (2%), confirming the spontaneous reduction of  $\text{Eu}^{3+}$  to  $\text{Eu}^{2+}$ . The spectrum acquired at 9.411 GHz consists of a number of resonance lines distributed over a wide magnetic field range from 5 to 500 mT, with an intense signal observed at 314 mT corresponding to  $g = 2.1$ , and additional strong lines corresponding to  $g = 5.6$  (120 mT) and  $g = 2.5$  (270 mT). This type of spectrum is commonly referred to as a “U spectrum” in view of its ubiquity for  $\text{Eu}^{2+}$  present in low concentrations in glassy hosts,<sup>18</sup> as well as in disordered polycrystalline materials.<sup>19</sup> At 34.122 GHz, the EPR spectrum reduces to a single absorption line centred at  $g = 2$ . The quantitative analysis of the spectra presented here is beyond the scope of this work and will be deferred to a later publication. Similar spectra have been observed for  $\text{LuP}_3\text{O}_9 : \text{Eu}$  (10%), but these spectra are not shown here.

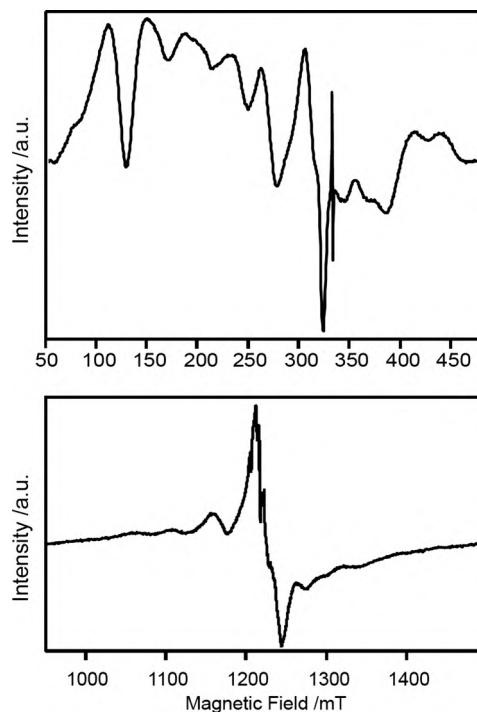


**Fig. 7** Continuous wave EPR spectra of  $\text{Eu}^{2+}$  in Eu-doped  $\text{LuP}_3\text{O}_9$ : (A) X-band (9.4 GHz) at 10 K and (B) Q-band (34 GHz) at 20 K. Experimental conditions: (A) microwave frequency, 9.411 GHz; microwave power, 2.0 mW; magnetic field modulation amplitude, 0.1 mT (100 kHz modulation frequency); time-constant: 81.92 ms. (B) microwave frequency, 34.122 GHz; microwave power, 0.41 mW; magnetic field modulation amplitude, 0.5 mT (100 kHz modulation frequency); time-constant: 10.24 ms. The first-derivative EPR spectra are sums over three accumulations each.

**Table 2** Fitting parameters of the  $^{151}\text{Eu}$  Mössbauer spectroscopic measurements of  $\text{LuP}_3\text{O}_9 : \text{Eu}$  (10% doping). Numbers in parentheses represent the statistical errors in the last digit;  $\delta$ , isomer shift;  $\Gamma$ , experimental line width

$T/\text{K}$	$\delta/\text{mm s}^{-1}$	$\Gamma/\text{mm s}^{-1}$
298	0.51(5)	2.83(17)
77	0.61(3)	2.70(8)
4	0.60(4)	2.73(11)

### 5.3 $^{151}\text{Eu}$ Mössbauer spectra of $\text{LuP}_3\text{O}_9 : \text{Eu}$

In order to have a sufficient amount of the Mössbauer spectroscopically-active element in the specimen, a sample with the nominal composition  $\text{LuP}_3\text{O}_9 : \text{Eu}$  (10%) was used for the  $^{151}\text{Eu}$  Mössbauer spectroscopic investigation. The spectra recorded at 4.2, 78 and 298 K are presented in Fig. 8, together with transmission integral fits. The corresponding fitting parameters are listed in Table 2. All spectra could be well reproduced with a single europium site at an isomer shift at around  $0.6 \text{ mm s}^{-1}$ , compatible with purely trivalent europium. Within the resolution, the spectra give no hint of a contribution from divalent europium. These signals would have been expected at around  $-10 \text{ mm s}^{-1}$ . The spectra were fitted without quadrupole splitting. The refined

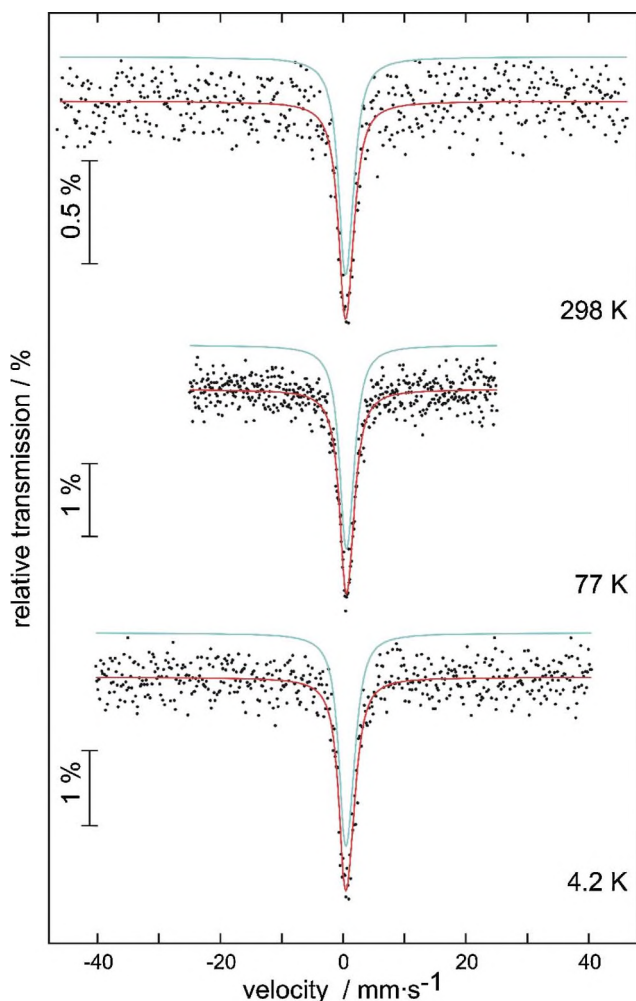


**Fig. 8** Experimental and simulated  $^{151}\text{Eu}$  Mössbauer spectra of  $\text{LuP}_3\text{O}_9 : \text{Eu}$  (10% doping) at different temperatures.

line width parameters are slightly enhanced when compared with the natural line width of europium. In view of the single rare earth site with a site symmetry of 1 in the  $\text{LuP}_3\text{O}_9$  structure, we can expect at least weak quadrupole splitting. This is hidden in the slightly increased line width. In such cases, a reliable independent refinement of both parameters is not stable. Thus, Mössbauer spectroscopy reveals the predominant presence of trivalent europium; a tiny content of divalent europium in the order of 1–2% may be present though.

### 5.4 Discussion of the measurements on $\text{LuP}_3\text{O}_9 : \text{Eu}$

The results of Mössbauer and EPR spectroscopy thus support our initially presented model of the *in situ* reduction of a minor part of the europium ions in  $\text{LuP}_3\text{O}_9 : \text{Eu}$ . EPR spectroscopy unequivocally proves the presence of  $\text{Eu}^{2+}$  while  $^{151}\text{Eu}$  Mössbauer spectroscopy proves the predominant presence of  $\text{Eu}^{3+}$ . In the luminescence spectrum, only an emission typical of  $\text{Eu}^{2+}$  could be found; this is in accordance with the fact that d–f transitions are allowed while f–f transitions are forbidden with respect to the parity selection rule. Therefore, the excitation energy will predominantly be emitted by the allowed and quicker emission *via* the divalent Eu ions.

## 6. Conclusions

In this contribution, we presented an investigation of the optical properties of  $\beta\text{-Y}(\text{PO}_3)_3 : \text{Eu}$ ,  $\text{Gd}(\text{PO}_3)_3 : \text{Eu}$  and  $\text{Lu}(\text{PO}_3)_3 : \text{Eu}$ . While the site size in the yttrium and gadolinium compounds is obviously sufficient to enable a simple statistical exchange of the host structure cation by trivalent europium, in the lutetium compound this is not straightforward. According to our model, the europium ions evade from the lutetium sites, which are six-fold coordinated, to interstitial voids that exhibit contacts to seven oxygen atoms. In these sites, the trivalent europium atoms are reduced to the divalent state, which could be proven by fluorescence and EPR spectroscopy. Predominantly, the europium ions maintain their trivalent state, as shown by  $^{151}\text{Eu}$  Mössbauer spectroscopy.

## Acknowledgements

The authors thank Prof. Dr H. Hillebrecht, Albert–Ludwigs–Universität Freiburg, for valuable discussions and generous support. Financial support by the Fonds der Chemischen Industrie (H. A. H.: Liebig Habilitationsstipendium, K. K.: Doktorandenstipendium) is gratefully acknowledged. This work was financially supported by the Deutsche Forschungsgemeinschaft (R. P. and I. S.). S. K. gratefully acknowledges Prof. Dr S. Weber, Albert–Ludwigs Universität Freiburg, for valuable discussions and continuous support.

## References

- 1 Review: H. A. Höpfe, *Angew. Chem., Int. Ed.*, 2009, **48**, 3572–3582 and references therein.
- 2 H. A. Höpfe and S. J. Sedlmaier, *Inorg. Chem.*, 2007, **46**, 3467–3474.
- 3 H. A. Höpfe, *J. Solid State Chem.*, 2009, **182**, 1786–1791.
- 4 H. van der Meer, *Acta Crystallogr., Sect. B: Struct. Crystallogr. Cryst. Chem.*, 1976, **32**, 2423.
- 5 E. Nakazawa, *J. Lumin.*, 2002, **100**, 89–96.

- 6 R. D. Shannon and C. T. Prewitt, *Acta Crystallogr., Sect. B: Struct. Crystallogr. Cryst. Chem.*, 1969, **25**, 925–946.
- 7 G. Blasse and A. Bril, *J. Chem. Phys.*, 1967, **47**, 5442.
- 8 P. Dorenbos, *J. Lumin.*, 2005, **111**, 89–104.
- 9 H. A. Höpfe, M. Daub and M. C. Bröhmer, *Chem. Mater.*, 2007, **19**, 6358–6362.
- 10 C. C. Lagos, *J. Electrochem. Soc.*, 1968, **115**, 1271–1274.
- 11 Z. Pei, Q. Su and J. Zhang, *J. Alloys Compd.*, 1993, **198**, 51–53.
- 12 K. Brandenburg and H. Putz, *DIAMOND*, Crystal Impact GbR, Bonn, Germany, 2008.
- 13 R. Hoppe, *Angew. Chem., Int. Ed. Engl.*, 1966, **5**, 95–106.
- 14 R. Hoppe, *Angew. Chem., Int. Ed. Engl.*, 1970, **9**, 25–34.
- 15 R. Hübenthal, *MAPLE: Program for the Calculation of the Madelung Part of Lattice Energy*, University of Gießen, Germany, 1993.
- 16 C. Wickleder, S. Zhang and H. Haeuseler, *Z. Kristallogr.*, 2005, **220**, 277–280.
- 17 A. Abragam and B. Bleaney, *Electron Paramagnetic Resonance of Transition Ions*, Oxford University Press, Oxford, 1970.
- 18 C. M. Brodbeck and L. E. Iton, *J. Chem. Phys.*, 1985, **83**, 4285–4299.
- 19 L. E. Iton, C. M. Brodbeck, S. L. Suib and G. D. Stucky, *J. Chem. Phys.*, 1983, **79**, 1185–1196.